

Supplement of Atmos. Chem. Phys., 21, 1191–1209, 2021  
<https://doi.org/10.5194/acp-21-1191-2021-supplement>  
© Author(s) 2021. This work is distributed under  
the Creative Commons Attribution 4.0 License.



*Supplement of*

## **Improvement of the satellite-derived $\text{NO}_x$ emissions on air quality modeling and its effect on ozone and secondary inorganic aerosol formation in the Yangtze River Delta, China**

**Yang Yang et al.**

*Correspondence to:* Yu Zhao (yuzhao@nju.edu.cn)

The copyright of individual parts of the supplement might differ from the CC BY 4.0 License.

**Number of tables: 4**

**Number of figures: 7**

### **Table list**

Table S1. Model performance statistics for meteorological parameters in the YRD region at the horizontal resolution of 9 km for January, April, July and October 2016.

Table S2. The summary of SNA observations collected and applied for AQM evaluation for the YRD region.

Table S3. The cases of sensitivity analysis of O<sub>3</sub> formation to its precursor emissions in the YRD region.

Table S4. The cases of sensitivity analysis of SNA formation to its precursor emissions in the YRD region.

### **Figure list**

Figure S1. The NO<sub>2</sub> TVCDs in July 2016 for the YRD region derived from POMINO v1. The map data provided by Resource and Environment Data Cloud Platform are freely available for academic use (<http://www.resdc.cn/data.aspx?DATAID=201>), © Institute of Geographic Sciences & Natural Resources Research, Chinese Academy of Sciences.

Figure S2. Scatter plots of the observed and simulated annual mean surface NO<sub>2</sub> concentrations with the bottom-up and top-down NO<sub>x</sub> emission estimates. The intercept was set to 0 when performing the regression.

Figure S3. The observed and simulated daily O<sub>3</sub> concentrations for the case of reducing 50% of BVOCs emissions for July 2016.

Figure S4. The observed and simulated hourly NO<sub>2</sub> and O<sub>3</sub> concentrations based on the bottom-up and top-down estimates of NO<sub>x</sub> emissions for July 2016 at JSPAES.

Figure S5. The observed and simulated hourly NH<sub>4</sub><sup>+</sup> concentrations based on the bottom-up and top-down estimates of NO<sub>x</sub> emissions for January, April, July and October 2016 at JSPAES.

Figure S6. The observed and simulated hourly SO<sub>4</sub><sup>2-</sup> concentrations based on the bottom-up and top-down estimates of NO<sub>x</sub> emissions for January, April, July and October 2016 at JSPAES.

Figure S7. The observed and simulated hourly SO<sub>2</sub> concentrations based on the bottom-up and top-down estimates of NO<sub>x</sub> emissions for January 2016 at JSPAES.

## Tables

Table S1. Model performance statistics for meteorological parameters in the YRD region at the horizontal resolution of 9 km for January, April, July and October 2016.

Variable	Statistics	January	April	July	October	Benchmark
Wind speed	Mean OBS (m/s)	2.59	2.51	2.39	2.56	
	Mean MOD (m/s)	2.76	2.65	2.51	2.71	
	Bias (m/s)	0.17	0.14	0.12	0.15	
	RMSE	0.47	0.42	0.49	0.42	$\leq 2.0^a$
	IOA	0.87	0.86	0.81	0.85	$\geq 0.6^a$
Wind direction	Mean OBS (°)	173.94	148.47	152.54	143.31	
	Mean MOD (°)	158.56	146.30	152.63	121.96	
	Bias (°)	-15.38	-2.18	0.09	-21.35	
	RMSE (°)	36.82	25.96	23.72	39.86	$\leq 44.7^b$
	IOA	0.81	0.85	0.85	0.78	
Temperature	Mean OBS (°C)	3.31	16.11	26.99	17.90	
	Mean MOD (°C)	3.95	16.62	27.31	19.02	
	Bias (°C)	0.65	0.51	0.33	1.12	
	RMSE (°C)	1.01	1.56	2.57	1.41	
	IOA	0.96	0.89	0.80	0.88	$\geq 0.8^a$
Relative humidity	Mean OBS (%)	72.96	73.69	76.15	81.03	
	Mean MOD (%)	70.19	79.92	82.63	86.35	
	Bias (%)	-2.78	6.24	6.48	5.32	
	RMSE	8.54	10.84	10.69	6.94	
	IOA	0.84	0.76	0.72	0.77	$\geq 0.6^a$

Note: <sup>a</sup> from Emery et al. (2001); <sup>b</sup> from Jiménez et al. (2006). OBS and SIM indicate the results from observation and simulation, respectively. The Bias, IOA and RMSE were calculated using following equations (P and O indicates the results from modeling prediction and observation, respectively):

$$Bias = \frac{1}{n} \sum_{i=1}^n (P_i - O_i); IOA = 1 - \frac{\sum_{i=1}^n (P_i - O_i)^2}{\sum_{i=1}^n \left( \left| P_i - \bar{O} \right| + \left| O_i - \bar{O} \right| \right)^2}; RMSE = \sqrt{\frac{1}{n} \sum_{i=1}^n (P_i - O_i)^2}$$

Table S2. The summary of SNA observations collected and applied for AQM evaluation for the YRD region.

Site	Location	Sampling period	Instrument/method	Temporal resolution	Reference
JSPAES	118.74°E, 32.05°N	January, April, July and October 2016	MARGA	Hourly	Unpublished
SORPES	118.95°E, 32.12°N	January, April, July and October 2016	MARGA	Daily	Ding et al., 2019
NUIST	118.70°E, 32.20°N	Mar 2016- Mar 2017	MARGA	Seasonal	Zhang, 2017
HZS	120.10°N, 30.20°N	Sep 2015-July 2016	Ion chromatography	Seasonal	Li, 2018
CZS	119.60°N, 31.72°N	July 2016-Aug 2016; Jan-Feb 2017	Ion chromatography	Seasonal	Liu et al., 2018
SZS	120.63°N, 31.30°N	Apr 2015; Aug-Sep 2015 Oct-Dec 2015	Ion chromatography	Seasonal	Wang et al., 2016

Table S3. The cases of sensitivity analysis of O<sub>3</sub> formation to its precursor emissions in the YRD region.

	NO <sub>x</sub> emissions	VOCs emissions
Case 1	-30%	No change
Case 2	No change	-30%
Case 3	-30%	-30%
Case 4	-30%	-60%
Case 5	-60%	-30%
Case 6	-60%	No change
Case 7	No change	-60%
Case 8	-60%	-60%

Table S4. The cases of sensitivity analysis of SNA formation to its precursor emissions in the YRD region.

	NO <sub>x</sub> emissions	SO <sub>2</sub> emissions	NH <sub>3</sub> emissions
Case 9	-30%	No change	No change
Case 10	No change	-30%	No change
Case 11	No change	No change	-30%
Case 12	-30%	-30%	-30%

## Figures

Figure S1. The NO<sub>2</sub> TVCDs in July 2016 for the YRD region derived from POMINO v1. The map data provided by Resource and Environment Data Cloud Platform are freely available for academic use (<http://www.resdc.cn/data.aspx?DATAID=201>), © Institute of Geographic Sciences & Natural Resources Research, Chinese Academy of Sciences.

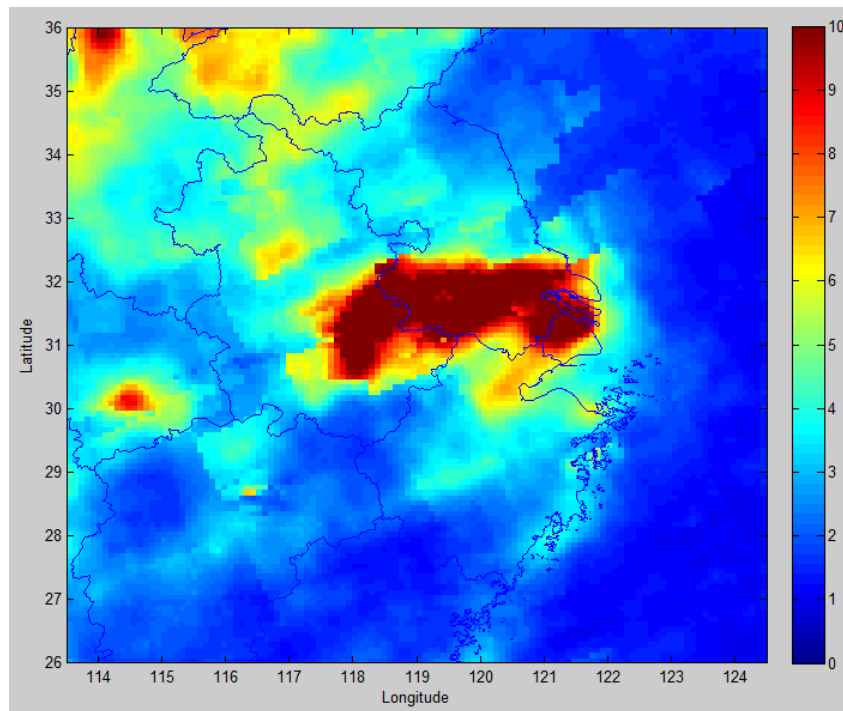


Figure S2. Scatter plots of the observed and simulated annual mean surface NO<sub>2</sub> concentrations with the bottom-up and top-down NO<sub>x</sub> emission estimates. The intercept was set to 0 when performing the regression.

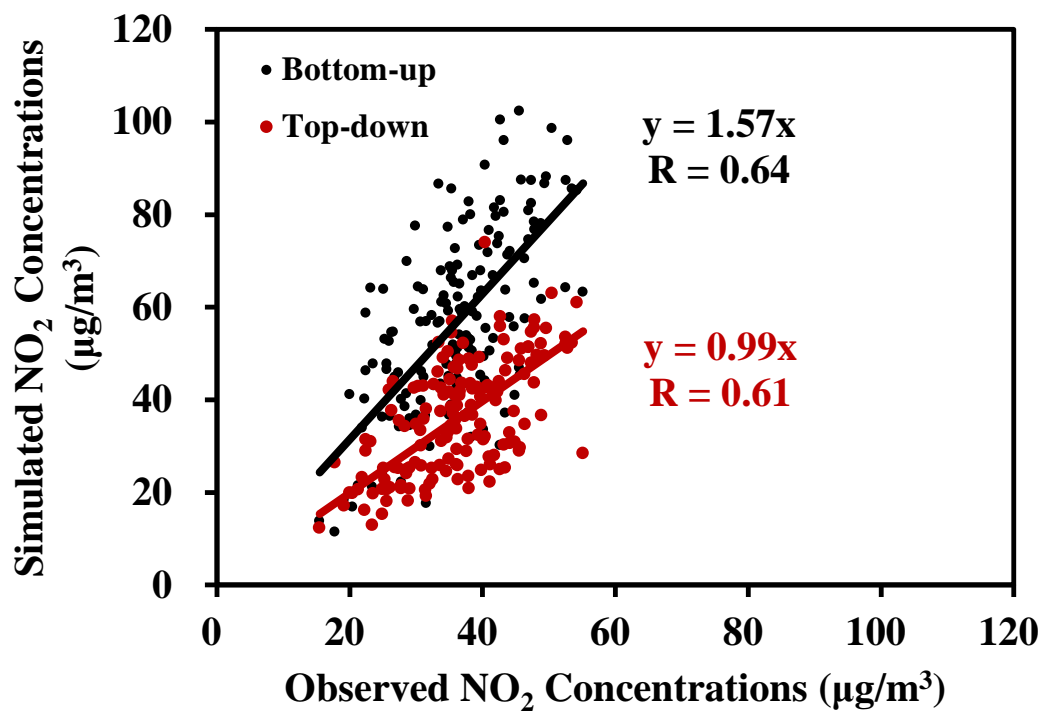




Figure S3. The observed and simulated daily O<sub>3</sub> concentrations for the case of reducing 50% of BVOCs emissions for July 2016.

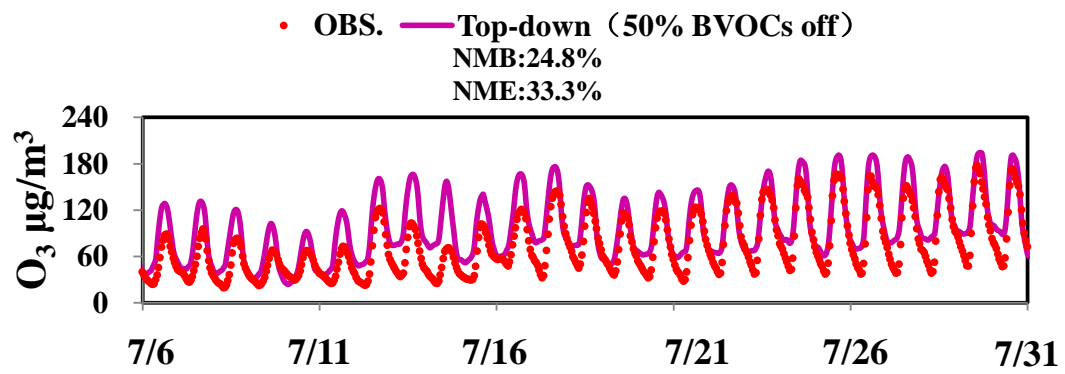
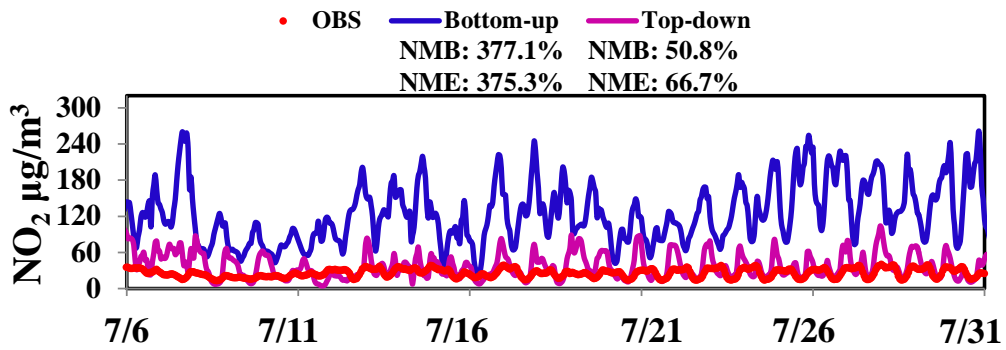
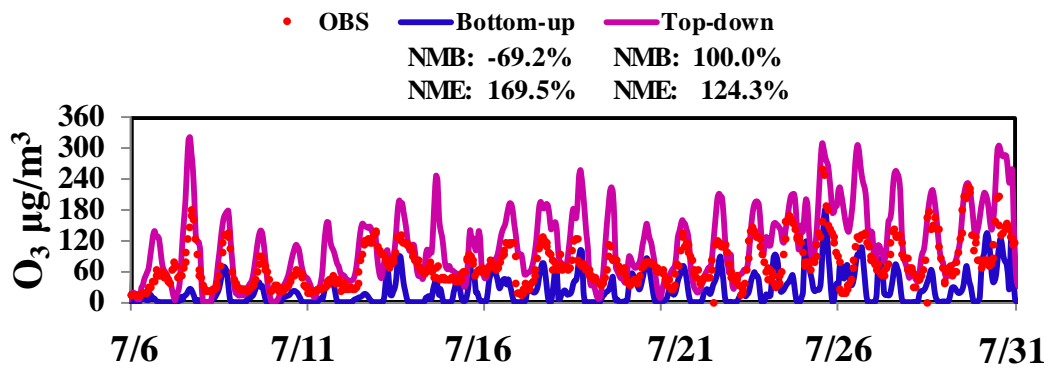


Figure S4. The observed and simulated hourly NO<sub>2</sub> and O<sub>3</sub> concentrations based on the bottom-up and top-down estimates of NO<sub>x</sub> emissions for July 2016 at JSPAES.



(a) NO<sub>2</sub> concentration



(b) O<sub>3</sub> concentration

Figure S5. The observed and simulated hourly  $\text{NH}_4^+$  concentrations based on the bottom-up and top-down estimates of  $\text{NO}_x$  emissions for January, April, July and October 2016 at JSPAES.

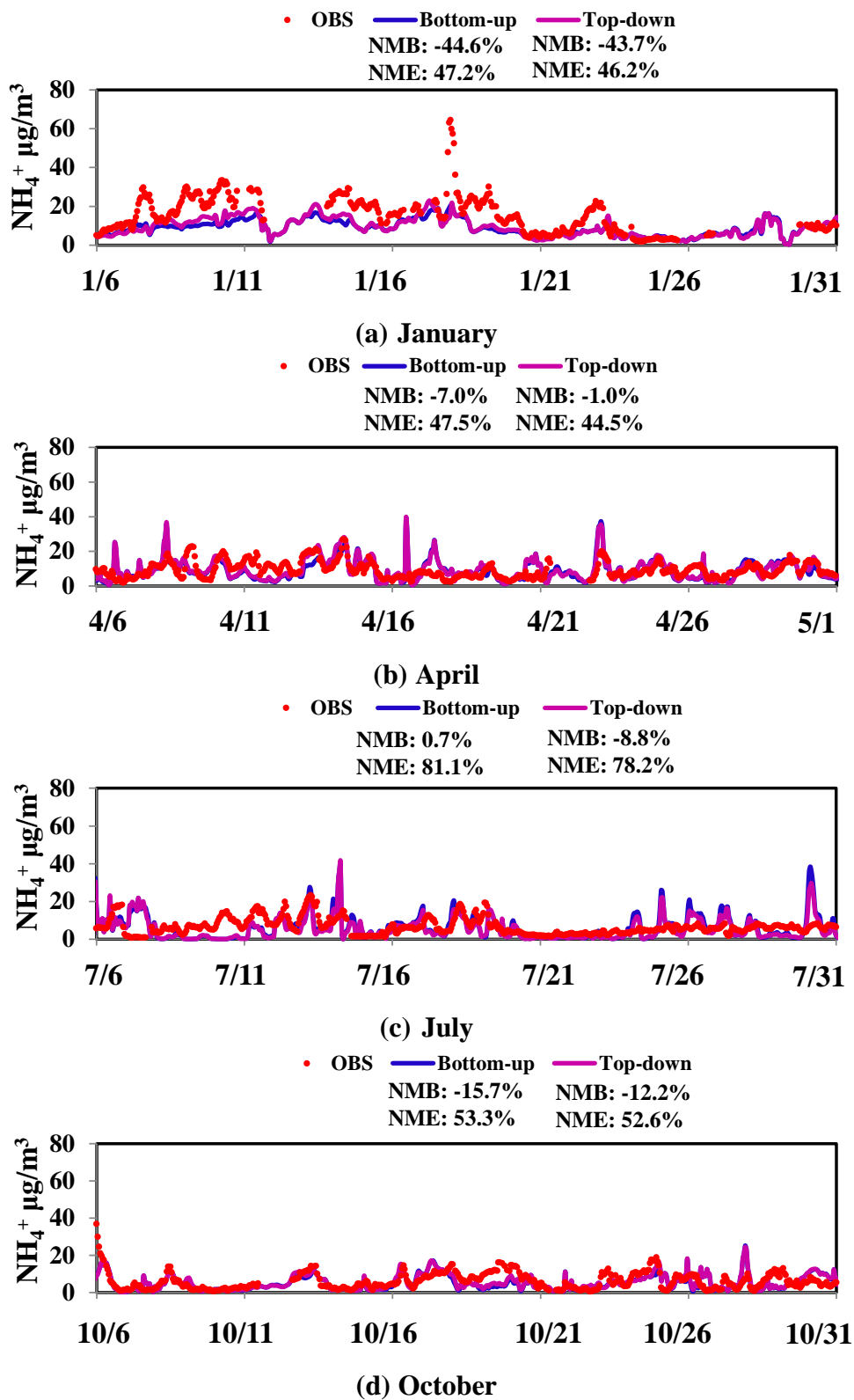
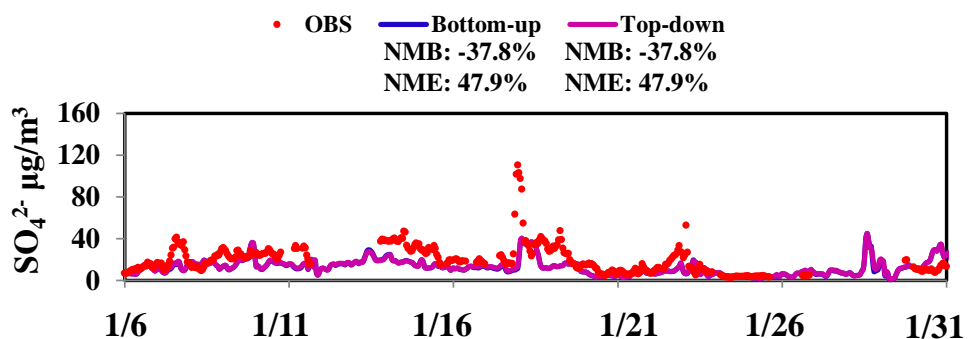
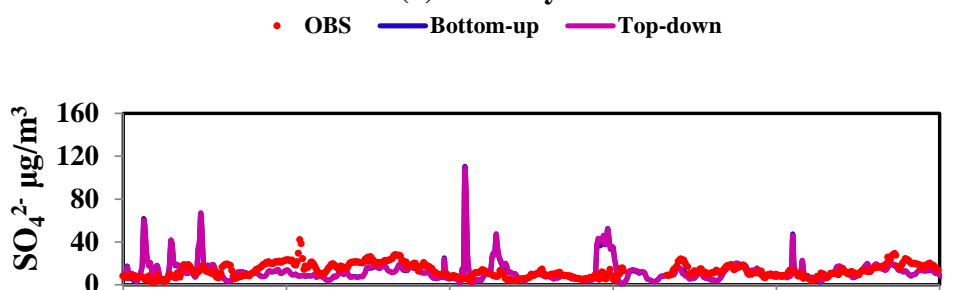


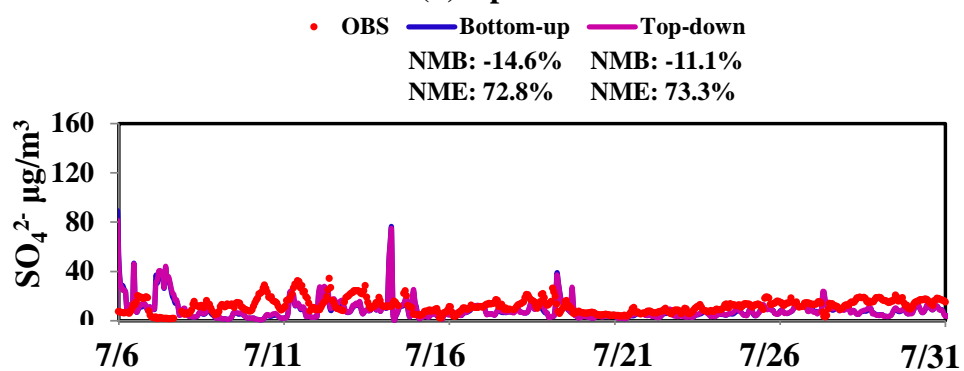
Figure S6. The observed and simulated hourly  $\text{SO}_4^{2-}$  concentrations based on the bottom-up and top-down estimates of  $\text{NO}_x$  emissions for January, April, July and October 2016 at JSPAES.



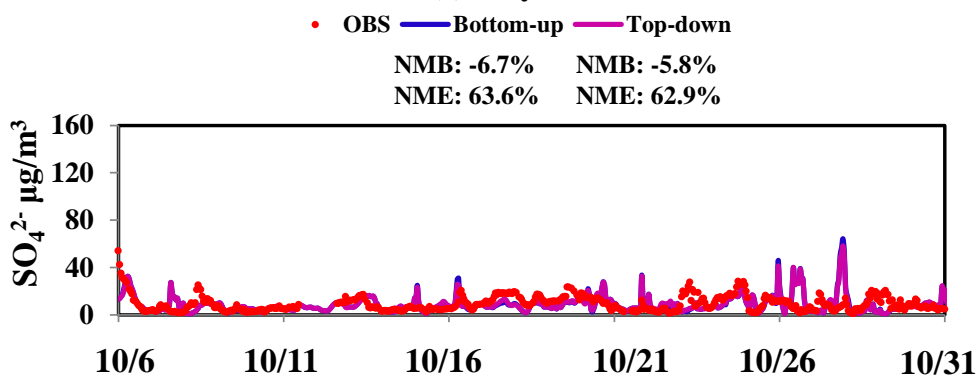
(a) January



(b) April

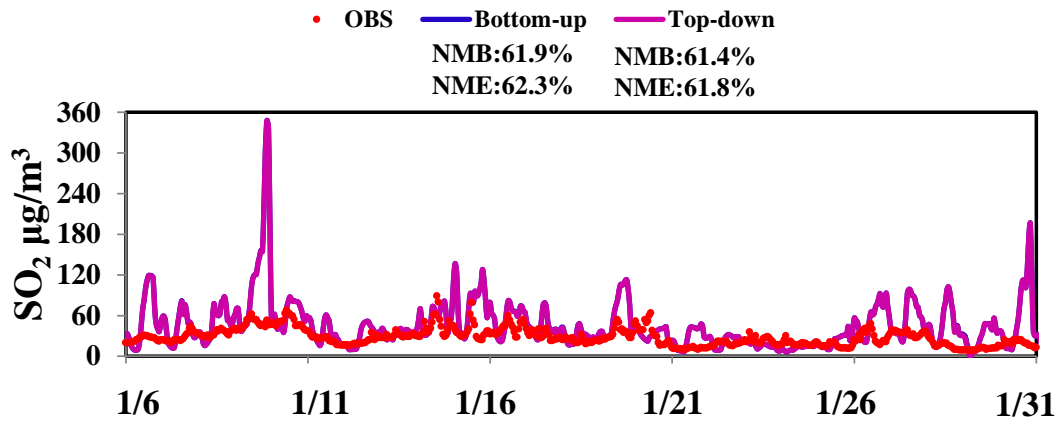


(c) July



(d) October

Figure S7. The observed and simulated hourly SO<sub>2</sub> concentrations based on the bottom-up and top-down estimates of NO<sub>x</sub> emissions for January 2016 at JSPAES.



## References

- Ding, A., Huang, X., Nie, W., Chi, X., Xu, Z., Zheng, L., Xu, Z., Xie, Y., Qi, X., Shen, Y., Sun, P., Wang, J., Wang, L., Sun, J., Yang, X., Qin, W., Zhang, X., Cheng, W., Liu, W., Pan, L., Fu, C.: Significant reduction of PM<sub>2.5</sub> in eastern China due to regional-scale emission control: evidence from SORPES in 2011–2018, *Atmos. Chem. Phys.*, 19, 11791–11801, 2019.
- Emery, C., Tai, E., and Yarwood, G.: Enhanced meteorological modeling and performance evaluation for two Texas episodes, Report to the Texas Natural Resources Conservation Commission, prepared by ENVIRON, International Corp, Novato, CA, 2001.
- Jiménez, P., Jorba, O., Parra R. and Baldasano J. M.: Evaluation of MM5-EMICAT2000-CMAQ performance and sensitivity in complex terrain: High-resolution application to the northeastern Iberian Peninsula, *Atmos. Environ.*, 40, 5056-5072, doi:10.1016/j.atmosenv.2005.12.060, 2006.
- Liu, J. S., Gu, Y., Ma, S. S., Su, Y. L., Ye, Z. L.: Day-night differences and source apportionment of inorganic components of PM<sub>2.5</sub> during summer-winter in Changzhou city (in Chinese), *Environ. Sci.*, 39, 980-989, 2018.
- Li, Z.: Seasonal pollution characteristics and cytotoxicity of PM<sub>2.5</sub> in district of Hangzhou City (in Chinese), Master thesis, Zhejiang University, Hangzhou, China, 2018.
- Wang, N. F., Chen, Y., Hao, Q. J., Wang, H. B., Yang, F. M., Zhao, Q., Bo, Y., He, K. B., Yao, Y. G.: Seasonal variation and source analysis on water-soluble ion of PM<sub>2.5</sub> in Suzhou (in Chinese), *Environ. Sci.*, 37, 4482-4489, 2016.
- Zhang, Y. Y.: Characteristic of water-soluble ions in PM<sub>2.5</sub> in the northern suburb of Nanjing based on on-line monitoring (in Chinese), Master thesis, Nanjing University of Information Science & Technology, Nanjing, China, 2017.